ECONOMICAL SOLUTIONS TO BLAST MITIGATION ON BRIDGES

By

AUSTIN DeROGATIS

Bachelor of Engineering, Civil Engineering
New Jersey Institute of Technology, 2007

Submitted to the Department of Civil and Environmental Engineering
in Partial Fulfillment of the Requirements for the Degree of

Master of Engineering in Civil and Environmental Engineering

at the

MASSACHUSETTS INSTITUTE OF TECHNOLOGY

JUNE 2008

Signature of Author: _____
Department of Civil and Environmental Engineering
May 9, 2008

Certified by: _____
Jerome J. Connor
Professor of Civil and Environmental Engineering
Thesis Supervisor

Accepted by: _____
Daniele Veneziano
Chairman, Departmental Committee for Graduate Studies

ECONOMICAL SOLUTIONS TO BLAST MITIGATION ON BRIDGES

By

AUSTIN DeROGATIS

Submitted to the Department of Civil and Environmental Engineering
on May 9th, 2008, in partial fulfillment of the
requirements for the Degree of Master of Engineering in
Civil and Environmental Engineering

Abstract

Mitigating the energy created from a blast has been a topic of utmost importance in the terrorism-feared world of today. Main targets of concern are passageways that are significant to a specific area, such as bridges. These structures are expensive to construct and vulnerable to explosive loads which is why a cost-effective means of blast mitigation must be researched.

There are many aspects of bridges that could be damaged when a blast load is applied. These susceptible areas can be strengthened using new-age, high-strength composite materials to ensure the security of the whole structure. These materials are able to sustain larger loads while dissipating higher amounts of energy when compared to conventional building materials. As a result, the response of the entire structure will be minimized when a blast load is applied. Despite the fact that these composites cost more than typical materials, the increase in project cost could be minimized by limiting the use of these high-strength materials for only the critical areas of the bridge.

Other cost effective solutions to blast mitigation occur in the preliminary design phase. Eliminating all pressure-amplifying areas would save members and connections should a blast occur. Also, designing a bridge with high vertical clearances above areas of excessive boat traffic would also minimize the resultant forces and stresses from an explosion.

Thesis Supervisor: Jerome J. Connor
Title: Professor of Civil and Environmental Engineering

Acknowledgements

I would like to thank the following people whose guidance made my Masters Degree at MIT possible.

My family for their support and motivation throughout my academic career.

Professor Connor, for his patience and willingness to answer any question at any time, regardless of his schedule.

MEng. Class of 2008 for always being there for me. It has been a pleasure working with you for the past year. Best of luck to you all.

Table of Contents

List of Figures

List of Tables

1 Introduction

In the post-9/11 world of today, intense interest has developed in blast resistant design for bridges. These blast loadings and the structural responses inherent should be researched, corrected, and implemented into all existing and newly constructed bridges. Using techniques that resolve the blast issue could be the difference between having a slight structural defect or a complete collapse. The only difficulty with alleviating this risk is the immense cost of the mechanisms necessary. As a result, a cost effective means for this security must be investigated.

One of the main considerations when investing a structure as a whole, is understanding its vulnerable areas. These danger zones should be examined with close scrutiny because one explosion could lead to a domino effect with the rest of the supports, thus allowing the entire bridge to collapse.

There are many economical techniques that are used to lower the risk of an attack on such an area, or alleviate the effect if such a blast should occur. One of the best methods for this security is optimal usage of newer, stronger materials. These highly researched materials are much stronger than conventional bridge materials and are therefore able to sustain larger loads while dissipating energy from a blast. Although these materials are more costly than standard ones, using them in critical bridge supports would greatly enhance the structural integrity of the entire structure. Other blast mitigation techniques, such as reducing confined areas and increasing the standoff distance from a blast, could be incorporated in the preliminary design stages of the bridge. Determining the most likely location of a blast could allow architects to design a bridge where the critical members are far from the initial explosion. Also, eliminating confined areas where blasts are magnified would greatly reduce the stresses throughout all of the structural components should a blast occur.

2 Problem

An explosion consists of transient air pressure waves produced by a rapid chemical reaction. This reaction creates intrusive blast waves which are constantly reflected by bridge components and redirected into others, creating an array of structural responses. The magnitude of the blast a member experiences depends on the type and quantity of the explosive materials along with the standoff distance from application (Mays and Smith, 1995). These dynamic effects cause individual members to fail thus risking the structural integrity of the entire structure. If the initial explosion is close enough to the bridge, shrapnel could impact the members, causing permanent deformations or cratering. Also, the increased temperatures from the explosion and the ensuing fires alter the properties of building materials and lead to failure. Overall, there are numerous

ways blast loads could negatively impact bridges, and proper usage of new-age materials along with clever design schemes could ease these problems.

3 Structural Analysis

There are many analytical methods for investigating explosive loads on structures. The most accurate and widely used analysis method is a single or multiple degree of freedom nonlinear dynamic analysis. These methods utilize Newtonian mechanics to break down physical systems into solvable mathematical equations. However for more complex systems, this equilibrium law is used in dynamic propagation software to determine structural responses for given loads. Once the data is compiled, one is able to estimate damage levels based on deformation criteria.

A more visual analytical method is finite element analysis (FEA). FEA uses computer modeling to apply loads or pressures onto a particular structural member and then analyzes the model for

specific results. This analysis uses equations of equilibrium on discrete regions of a structure to construct a series of simultaneous equations. These simultaneous equations are then solved utilizing matrices and laws of linear algebra while creating an output of structure reaction.

These analysis techniques will be investigated throughout the rest of this paper to form conclusions about blast loading and a structure's respective responses. General laws of physics, chemistry, and calculus were also applied to assess the effects of impulse loads.

4 Blast Design- Terrorism

Terror-proofing bridges is a very difficult task that requires in-depth research in various fields. The design criterion for a specific bridge is based on its importance deciphered through a vulnerability evaluation, and will enable researchers to categorize a bridge's inherent danger. The given standards institute a guideline threat level and identify acceptable levels of damage with the particular loading conditions. The design loads are determined by using the worst possible explosion for each structural component. For example, a certain predetermined blast is projected downward for footing design, while for column design, the blast will be projected laterally. This will allow each element, and the structure as a whole, to withstand a typical blast

regardless of how it is applied. A list of the performance base standards for bridges is as follows (Winget, Marchand, and Williamson, 2005).

Table 1- Performance Based Standards for Bridges [1]

Category 1 (very important)
Concept: East structural element is designed to withstand 2 separate cases: large loads with repairable damage, and smaller loads with negligible damage
Design loads- Case 1 (small loads)
"Most-likely" treat scenarios using the following at worst possible locations for each structural element being designed:
Midsize truck bomb
Midsized hand emplaced explosive scenarios
Midsized static load for vehicle impact scenarios
Acceptable damage- Case 1 (small loads)
Local deck failure; support system still intact with negligible damage; truss/cables/piers still capable of supporting design loads when considering structural redundancy; no unrepairable foundation instabilities and no span loss; steel girders <5% maximum deflection to length ration, reinforced concrete girders <4%.
Design loads- Case 2 (large loads)
"Most-likely" threat scenarios using the following at worst possible locations for each structural element being designed
Large truck bomb
Large hand-emplaced explosive scenarios
Large static load for vehicle impact scenarios
Acceptable damage- Case 2 (large loads)
Local deck failure; support system still intact with minor damage; not capable of supporting design loads but easily repairable; no unrepairable foundation instabilities and no span loss; steel girders <12% maximum deflection to length ratio, reinforced concrete girders <8%
Category 2 (important)
Concept: Designed to withstand smaller loads with repairable damage.
Design loads- Same as Category 1, Case 1
Acceptable damage- Same as Category 1, Case 2
Category 3 (slightly important)
Concept: Designed to withstand smaller loads with no more than one span loss.
Design loads- Same as Category 1, Case 1
Acceptable damage- no more than one span loss (no progressive collapse)
Category 4 (unimportant)
No standard

The most important step in a threat analysis is to identify all possible courses of action against a particular type of bridge and the level of destruction intent of the bomber. For the bridge in construction, an evaluation and rank of the terrorists' most likely means of attack should be assembled, as seen in Figure 1. This process is most efficiently developed through a multiplication decision matrix, where each criterion is designated a weight based on its importance to the terrorist. This is done for each course of action where the criterion could then be assigned a relative score. A general probability can then be deciphered from the analysis and the criterion with the higher score will be used as the main basis for design.

The final step in a threat analysis is deciding on whether or not a bridge design should incorporate the certain countermeasures necessary to mitigate a predicted blast. Typically, senior leadership opts to save money and continue construction without redesigning for possible attacks while just accepting the inherent risks of the bridge. For this reason, cost efficient blast mitigation should be researched and incorporated into general bridge construction (Williamson and Wingett, 2007).

Diagram	Weapon	Location	Desired Effects
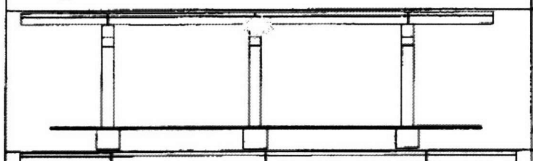	Hand placed explosives	At girder supports	Destroy supports, collapse 2 spans
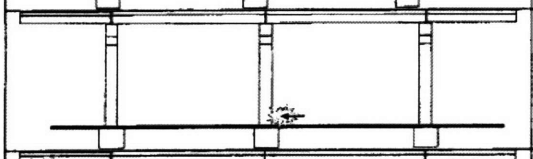	Hand placed explosives	At column base directed towards column	Destroy column near base, damage footing, create crater, collapse 2 spans
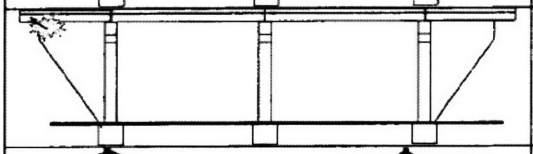	Hand placed explosives	On abutment seat	Destroy abutment and collapse 1 span
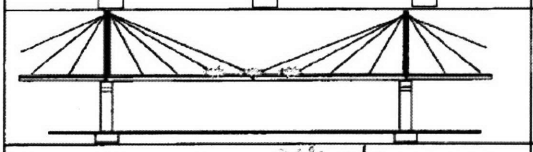	Hand placed explosives	Cable anchorages	Destroy anchorages and collapse 1 or more spans
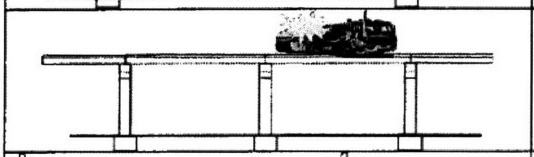	Fuel tanker/truck bomb	On deck	Destroy deck, spall girders, subject bridge to sustained fire, collapse 1 or more spans
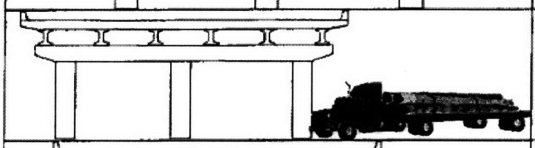	Large truck	Into column	Destroy column, possible fire, collapse 2 spans
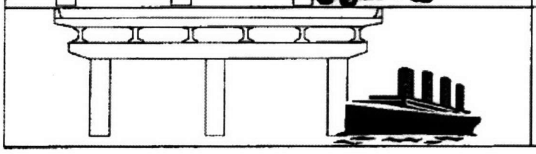	Ship/barge	Into pier	Destroy pier, collapse 1 or more spans

Figure 1- List of Possible Terrorist Treat Courses of Action [2]

4.1 Materials

For terrorism design, a main area of research is in developing more resilient materials. There are many materials being tested that can withstand and dissipate a blast's energy to minimize damage on bridge members. The cost of these materials is typically more expensive than conventional means; however, using them at strategic locations could protect vulnerable points of a structure while maintaining a low cost.

4.1.1 Foam Cladding

Metallic foams are lightweight materials with the ability to absorb large amounts of energy. The foam cladding is typically constructed as a layered composite structure containing a foam panel with a surrounding metallic plate. This arrangement forces the overpressure created from a blast to dissipate to a much lower magnitude, thus reducing the response of the structure (Ye and Ma, 2007).

4.1.2 Ultrahigh-Strength Concrete

Utilizing ultra high-strength (UHS) concrete on critical areas of structures could greatly enhance the overall stability when a blast is applied. This material could aid in anti-terrorism design since it contains a fire-resistant composition along with a compressive strength four times greater than conventional building concrete. Although the cost of this material is higher than typical concrete, the cross-sectional areas will be lessened, thus reducing the amount of necessary material (Lee, 2007).

4.1.3 Fiber Reinforcing

Fiber-reinforced concrete is a lightweight material that is structurally efficient. The composite material is comprised of carbon reinforcing fabrics surrounded by an epoxy resin matrix. This

composition is over 500 times more resistant to cracking while being more than twice as ductile as conventional concrete. Fiber-reinforced concrete has become increasingly popular in construction in recent years and is expected to be more prevalent in the years to come (Chen and Chung, 1993).

4.1.4 Concrete-Filled, Fire-Resistant Steel

Concrete-filled steel-tube (CFST) members are able to sustain high loads, while having an incredible resistance to fire when compared to typical, hollow steel-tube members. Alone, concrete decreases in stiffness and compressive strength when subject to elevated temperatures. It also experiences odd thermal expansion behavior due to the rapid drying and mechanical loadings that blasts generate (William, Lee, Lee, and Xi, 2006). When steel encounters high temperatures, the material properties deteriorate which could potentially lead to member failure. The main reasons for failure are creep, a significant decrease in yield strength, and elongation. For these reasons, investigating a concrete-steel composite, along with using fire-resistant steel and fireproof coatings, is of utmost importance when dealing with terror-proof design (Han, Huo, and Wang, 2007). Charts depicting the tendencies of steel when heated are found in Appendix A.

4.2 Analysis of Materials

4.2.1 Foam Cladding

For this experiment, a dynamic analysis is used to demonstrate the importance of foam cladding while experiencing an explosive load.

A blast pressure can be approximated by a triangular pulse and is represented in the following set of equations, where p_0 is the initial peak pressure and t is the loading duration.

$$p(t) = \begin{cases} p_0(1 - t/t_0) & \text{for } t \leq t_0 \\ 0 & \text{for } t > t_0 \end{cases}$$

Using an elastic analysis with this composite material, a common bridge component (beam, plate, shell, etc.) can be modeled as a single degree of freedom system while incorporating equivalent load (C_l), stiffness (C_s), and mass (C_m) factors. Therefore a refined version of the equation of motion can be presented as:

$$C_m m\ddot{y} + C_s k y = C_l p(t) A$$

where m= total mass, k= total stiffness, p(t)= exerted uniform pressure on structure, A= exposed area bearing blast load. To simplify the equation, one can define a load-mass factor $C_{lm}=C_m/C_l$. because the stiffness and load factors are usually equivalent, $C_s=C_l$. Also, an equivalent mass can be defined as $m_{se}=C_{lm}m$. Using these parameters to manipulate the previous equation of motion gives the following equation for an elastic equivalent system.

$$m_{se}\ddot{y} + k y = p(t) A$$

However, considering the interaction between the foam cladding and the structure, one can come up with the equation of motion as follows. This derivation and free-body diagram are represented in Appendix B.

$$[m_1 + m_f + m_{se}]\ddot{y} + k y - p(t)A = 0$$

Now, using this equation of motion and certain parameters of the foam material, plots investigating the effects of an explosion can be constructed. The following graphs demonstrate non-dimensional deformation of the foam cladding and the non-dimensional deflection of the entire structure when a blast was applied. T denotes natural period of an equivalent structure.

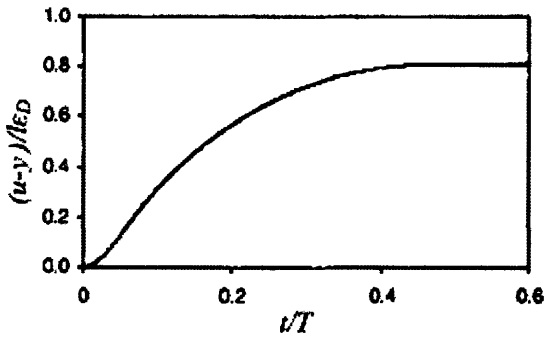

Figure 2- N-D Deformation of Foam Cladding [3]

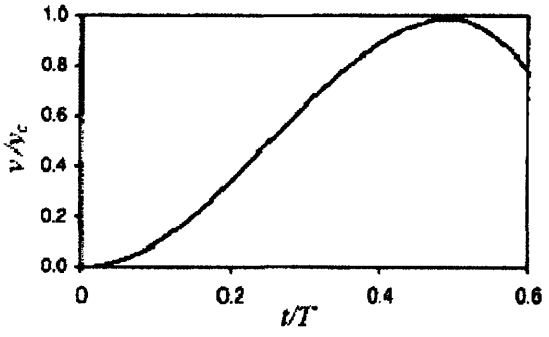

Figure 3- N-D Deflection of Structure [3]

From Figure 2, it can be observed that the foam layer undergoes a large plastic deformation from the inherent blast load. Also, as can be seen from Figure 3, the transmitted pressure from the foam causes the structure to deform. However, the deflection and velocity experienced from the mass are relatively small compared to those of the cover plate of the foam cladding. In this study, the deflection of the mass was approximately 1 cm while its velocity was about 5 m/s. The displacement and velocity of the cover plate of the foam cladding were approximately 5 cm and 50 m/s, respectively. It can then be concluded that the foam cladding absorbs the majority of the impact, thus allowing the structure to encounter larger blast loads, while only experiencing a fraction of the effects. (Ye and Ma, 2007)

4.2.2 Ultrahigh-Strength Concrete

The following test compares the blast effects of 6 tons of TNT onto a 1000x2000x100 mm slab of UHSC and a 1000x2000x100 mm slab of normal strength concrete (NSC) at a standoff

distance of 40 m. The UHSC panel contained prestressed tendons located centrally in the longitudinal direction. The NSC panel was reinforced with N16 bars at 200 mm center-to-center.

When tested, the UHSC panel yielded only minor vertical cracks (.1 mm) while showing neither crushing nor spalling. During the blast, the maximum midspan inward deflection was measured to be 27.1 mm while the maximum outward deflection was measured to be 20.7 mm. Therefore the test demonstrated only minor damage occurring to the panel.

When the blast was applied to the NSC specimen, panel failure due to concrete breach was noticed. The front face of the concrete was crushed while yielding a vertical crater with a width of 100 mm and a depth of 30 mm. The specimen also presented a permanent 142 mm vertical deflection. At the rear surface, an 8 mm wide crack was measured at midspan while the concrete cover spalled off. Overall, the failures presented through the test demonstrated severe damage to the NSC panel. Figures 4 and 5 demonstrate the concrete panels after experiencing the blast load.

Figure 4- UHSC Panel After Blast [4]

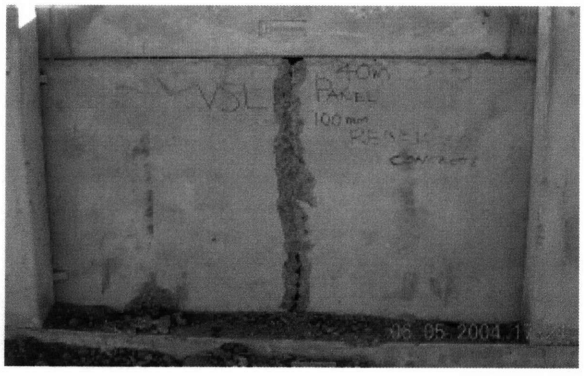

Figure 5- NSC Panel After Blast [4]

The next test investigated the two concretes' respective responses at very high strain rates. Therefore, a series of tests was conducted on large diameter cylinders to achieve a range of

loading rates and a plot of the particular material's stress/strain characteristics. In order to create this plot, one first needs to discover the dynamic increase factor (DIF) characteristic for the two concretes. The DIF is a ratio of the static compressive strength to the dynamic peak stress. The wide range of loading rates enables one to create an accurate plot of how the material will act when a blast is applied. This graph is shown in Figure 6.

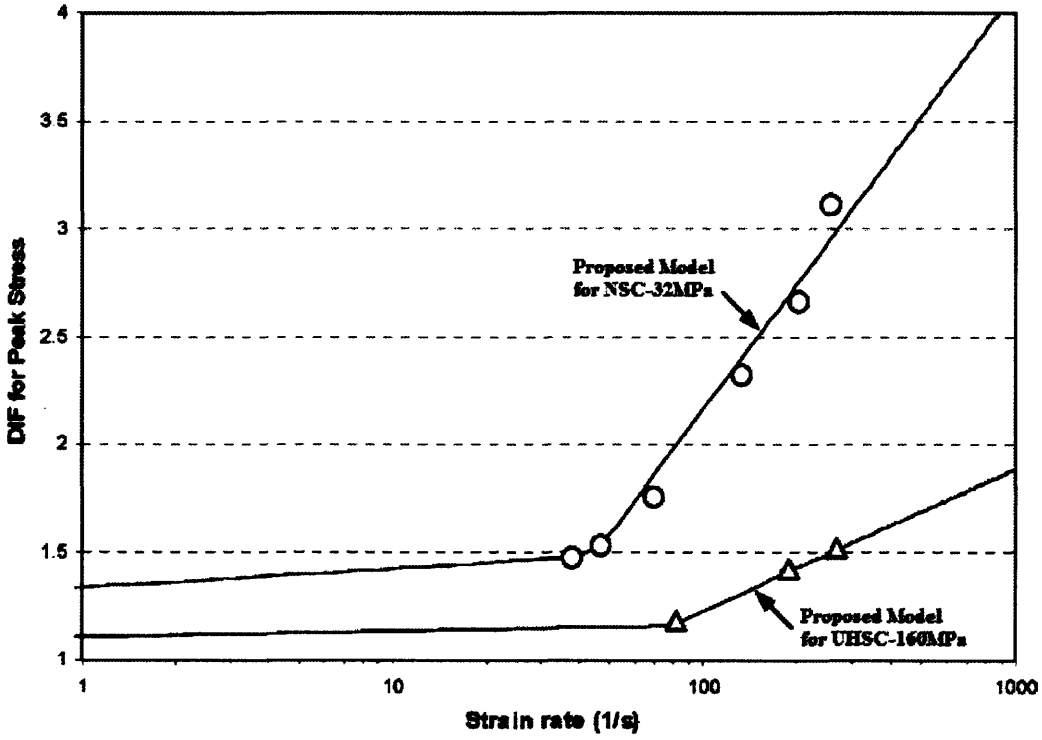

Figure 6- DIF vs. Strain Rate [4]

As can be seen from the above graph, the UHSC is less rate sensitive than the NSC. This proves that the UHSC will be able to sustain less damage for loads that are applied in a quick, impulsive manner (Ngo, Mendis, and Krauthammer, 2007).

4.2.3 Fiber Reinforcing

The testing for this composite material used panels comprised of plain autoclated aerated concrete (P/AAC) and fiber reinforced polymer autoclated aerated concrete (FRP/AAC). Three

specimens of each case were examined in this impact loading experiment setting the thickness as the only variable. The load cell in the test was rated for a maximum load of 44 kN while a drop height of 40 cm was used for each test. This combination of weight and height for the striker assembly created a loading condition which was close to the calculated maximum allowed by the specimens before failure. Once the load was applied onto the concrete panels, load versus time data along with impact velocity magnitudes were measured from software. Other variables were solved via the following laws of physics:

$$f(t) = mg - p(t) \tag{1}$$

$$a(t) = \frac{f(t)}{m} = \frac{g - p(t)}{m} \tag{2}$$

$$v(t) = \int_0^t a(t)dt = gt - (1/m)\int_0^t p(t)dt \tag{3}$$

$$x(t) = \int_0^t v(t)dt = v_i t + 0.5gt^2 - 1/m \int_0^t \int_0^t p(t)dt \tag{4}$$

$$E(t) = K(t) + v(t) + E_a(t) = constant \tag{5}$$

$$E_a(t) = (m/2)(v_i^2 - v(t)^2) + mgx(t) \tag{6}$$

where p(t)= load value measured by software at time t, m= hammer mass, g= gravitational acceleration, f(t)= total force acting on hammer, a(t)= resultant acceleration of hammer, v(t)= velocity of hammer, x(t)= position (deflection) of hammer, K(t)= kinetic energy of hammer, E_a= energy absorbed by the specimen, and E(t)= total energy of the hammer/specimen system.

Once these values were obtained, Table 2 was constructed comparing the two different specimens tested.

Table 2- Plain Concrete vs. FRC Impact Test [5]

Specimen	Thickness (mm)	Peak load (kN)	Max. deflection at midspan (mm)	Total Energy (joule)
P-AAC	25.4	7.18	1.61	6.33
P-AAC	50.8	10.30	1.72	10.26
P-AAC	76.2	21.07	1.84	18.36
FRP/AAC	25.4	13.65	1.75	15.11
FRP/AAC	50.8	16.93	2.05	21.41
FRP/AAC	76.2	23.39	2.27	66.56

As can be observed from the table, the FRP concrete was able to absorb more energy from the impulse load created by the hammer. The fiber reinforcement allowed the specimens to attain higher peak loading for each case when compared to the plain concrete panels with the same thicknesses. The higher load attained by the FRP, along with the larger deflection, proves that this composite material is not only stronger, but also more ductile than the plain concrete. The fiber reinforcement allows the panel to deflect more without failing like the conventional, brittle concrete. As a result, this reinforcement will be able to dissipate a blast load more efficiently than the unreinforced concrete. This conclusion can be more clearly seen by the load vs. time and energy vs. time graphs as follows in Figure 7 (Uddin, Shelar, and Fouad, 2006).

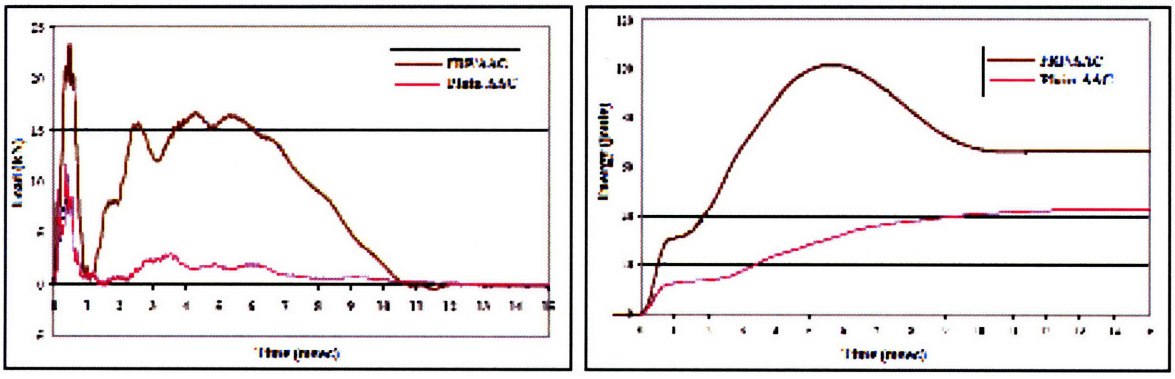

Figure 7- Comparison Graphs of FRP AAC and Plain AAC [5]

4.2.4 Concrete-Filled, Fire-Resistant Steel

To analyze this composite material, concrete-filled, fire-resistant steel (FR) tubes were tested against concrete-filled, ordinary steel tubes while experiencing a dramatic increase in temperature. The FR and ordinary steel tubes each contained the same dimensions (height= 3.5 m, width= .3 m, and thickness= 9 mm). Table 3 demonstrates the heating results of steel tubes only.

Table 3- Mechanical Properties of Conventional Steel vs. FR-Steel [6]

Steel Type	Temperature (°C)	Proof Stress (MPa)	Tensile Strength (MPa)	Elongation (%)
Conventional Steel	Room	360.9	527.6	24
Conventional Steel	600	131.4	195.2	60
FR-Steel	Room	357.9	534.5	24
FR-Steel	600	217.7	323.6	46

As can be seen from the test results, the fire resistant steel yielded essentially the same results as the conventional steel when tested at room temperature. However, when the steel was heated to 600 °C, the FR-Steel was able to sustain higher loads while experiencing less elongation. The greater deformation and less load capacity create disasters for bridges subjected to these temperature conditions. When this special steel is used, individual members are protected while distributing less stresses and strains through other components of the bridge.

In order to investigate the heating effects on members more deeply, a new test was performed where the two steel materials were covered with a fire protective layer and filled with normal strength concrete. The FR-steel and concrete composition was tested for three cases: without protection, with ceramic protection, and with intumescent coating. The conventional steel and concrete sections were only tested with a thicker coating of the ceramic protection and then

compared to the FR-steel results. The results for this test are presented in Appendix C. After viewing data from the experiment, the concrete-filled steel and FR-steel combination with ceramic protection failed after 166 minutes of heating. The concrete-filled ordinary steel tubes with an extra layer of ceramic protection failed after 194 minutes. Also, the testing of the FR-steel yielded an elongation of 16.7 mm while the heavily coated ordinary steel tube only elongated 10.8 mm. These results prove that the fire protective coating is more efficient at resisting the heat and maintaining the material properties of the composite than the FR-steel. The best case scenario for preventing failure from a fire would be a combination of fire-resistant steel with a thick layer of ceramic coating (Sakumoto, Okada, Yoshida, and Tasaka, 1994).

5 Blast Design- Accidents

Blast loads can be applied on bridges through means other than terrorism, such as boater and vehicular accidents. Since vehicle accidents usually occur above the deck and structures are constructed to sustain high gravity and lateral loads, the main source of blast proofing these mishaps are discussed in the materials section. However, boater accidents occur below deck, and since bridges are not typically built to sustain high uplift pressures throughout every component, there are many inherent dangers. Sub-deck blasts impose threats on individual components and members, along with the structure as a whole.

5.1 Confined Areas

When a blast occurs beneath the deck of a bridge, large uplift forces act on the structural members. These explosions can be magnified in confined regions of the bridge, usually where the bridge connects to land or between girders as presented in the following figures.

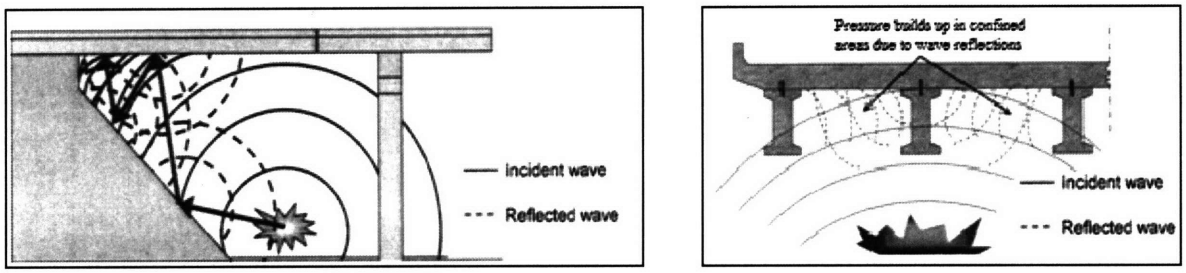

Figure 8- Confinement Effects [1]

The magnitude of the damage to the members depends on the initial size of the blast, along with the area over which it is applied. Below-deck blasts in confined areas are known to assist in the failure of the following structural components:

5.1.1 Shear Connectors

This intense pressure buildup causes failure of shear connectors which will allow the deck to separate from the main support girders. As a result, localized deck failures will ensue.

5.1.2 Girders

Girder response to impact loading could result in a variety of structural failures, especially when a blast is directed into a confined area between main girders. Concrete can be deteriorated through spalling or cratering. Spalling is where shock waves traveling through the members create tension spots in areas that are not reinforced to withstand the inherent tensile forces. Cratering occurs from intense forces hitting the face of a member directly, thus causing fragments to be removed. Both cases put the structural integrity of the bridge at risk.

5.1.3 Columns

Similar to girders, columns could result in large deformations, shear, or flexural failures when a blast is applied. These effects are only magnified when the columns are arranged in a way that creates confined regions. Cratering and spalling are common damage elements, and since these columns carry excessive vertical loads, they could lead to failure on a larger scale (Winget, Marchand, and Willamson, 2005).

5.2 Vertical Clearance

The standoff distance for any structure determines the magnitude of the pressure which it will experience from a given explosion. When blasts occur below the bridge deck, many important components are affected. The further these components are from the blast, the less chance they have of failing, thus protecting the structure as a whole. Bridges that have high vertical clearances also have low probability of member failure due to marine explosions (McCallen, Wattenburg, Lewis and Mote).

5.3 Analysis of Accidents

5.3.1 Confined Areas

When analyzing the blast effects onto a confined area and a non-confined area, one must consider the dimensions of the configuration. For this analysis, the dimensions defined in Figure 9 will be used (assume unit depth).

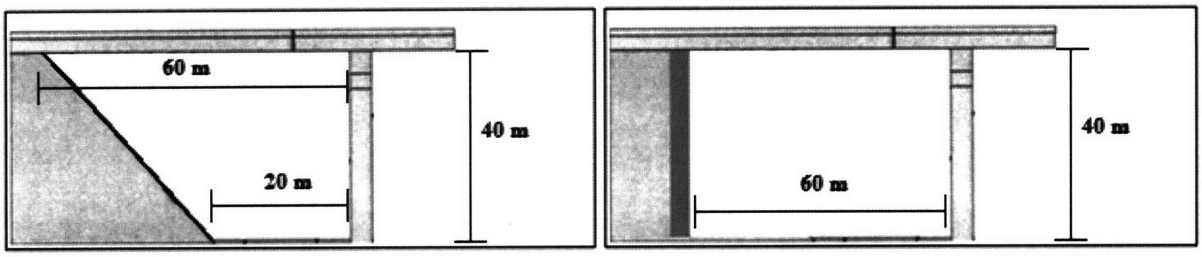

Figure 9- Dimensions of Confined Area vs. Retaining Wall Area (adapted from [1])

The volume of the confined area (picture on the left) is 1600 m^3 (V_1) while the volume of the diagram with the retaining wall is 2400 m^3 (V_2). Now, by rearranging Boyle's law to get the equation: $P_2=P_1V_1/ V_2$, and assuming the blast pressure produced in the confined side (P_1) to be 900 kN/m^2, a blast of the same magnitude would only produce a pressure of 600 kN/m^2 onto the bridge with the retaining wall. This reduction in pressure not only decreases the amount of deflection experienced by the main beam, but also decreases the stresses and deformations realized by the individual components (Winget, Marchand, and Williamson, 2005).

5.3.2 Vertical Clearance

The following analysis was performed via finite element software, ADINA, and was a simulation of a boat explosion onto a W14x90 beam. The beam was modeled as fixed on one end and supported by a roller on the other, thus replicating a simple bridge configuration. The magnitude of the explosion was equivalent to 22,241 N of TNT applied at specified distances away from the target so a deflection and moment trend can be investigated for each case. The model developed is a line beam, 3 meters in length, which contains the properties and cross-section of the W14x90 beam. For each of the tests, the material properties were held constant (n= .25, E= 7e10 N/m^2, and I= 4.16e-4 m^4). Figure 10 demonstrates the beam model used for analysis.

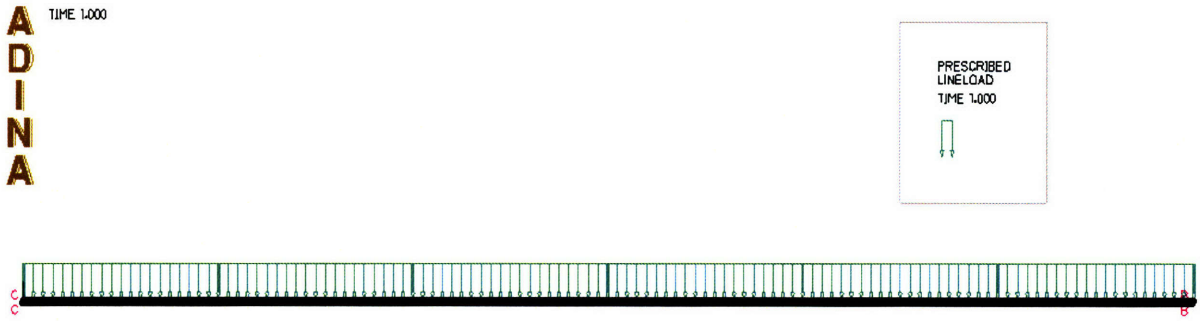

Figure 10- FEA Beam Model (L=3m)

5.3.2.1 Case A: Explosion applied 15.25 m from target

The distance investigated from this blast condition would create a pressure of 896,319 N/ m^2 onto the upper flange of the beam. This load produces a maximum deflection of 5.05 mm along with a maximum moment of magnitude 371,058 N-m. The following figures 11 and 12 represent the deflection and moment profiles, respectively.

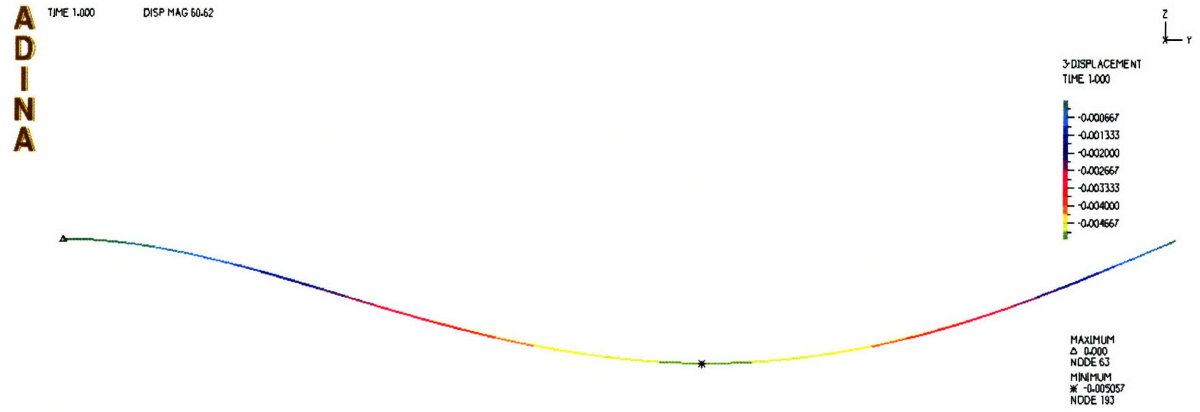

Figure 11- Deflection Profile (15.25 m)

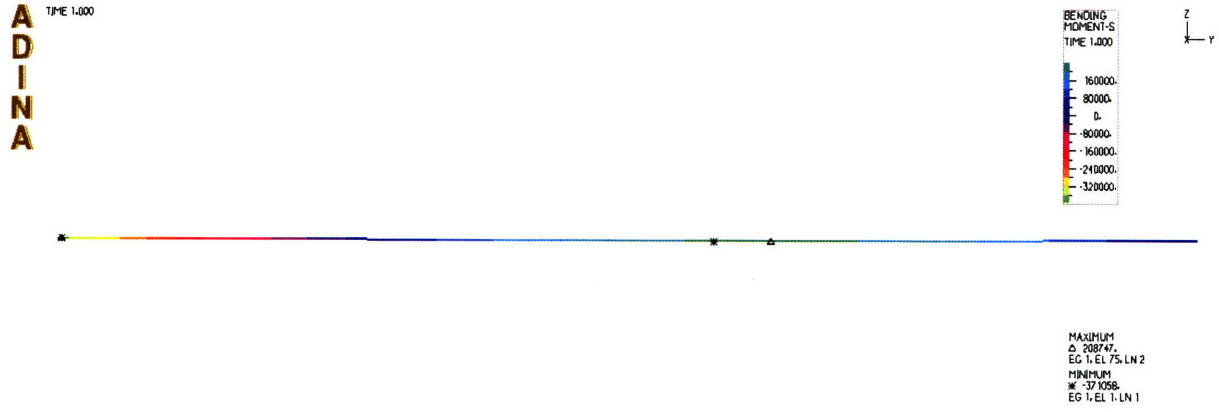

Figure 12- Moment Profile (15.25 m)

5.3.2.2 Case B: Explosion applied 30.5 m from target

The distance investigated from this blast condition would create a pressure of 206,843 N/ m^2 onto the upper flange of the beam. This load produces a maximum deflection of 1.07 mm along with a maximum moment of magnitude 85,629 N-m. Figures 13 and 14 represent the deflection and moment profiles, respectively.

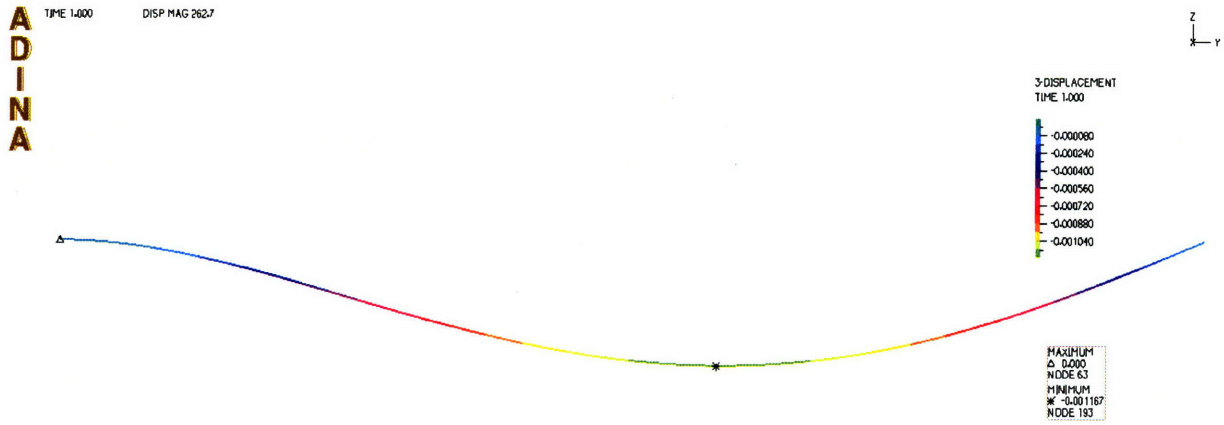

Figure 13- Deflection Profile (30.5m)

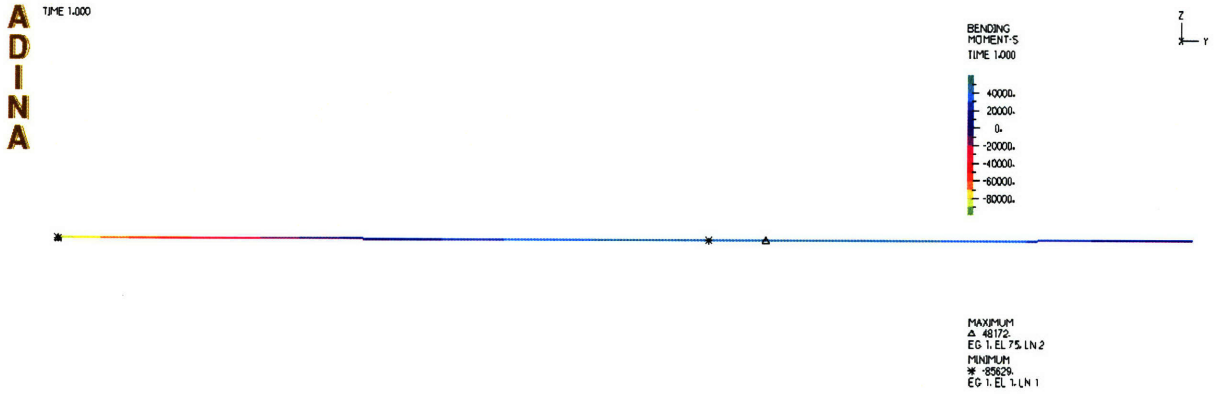

Figure 14- Moment Profile (30.5 m)

5.3.2.3 Case C: Explosion applied 61.0 m from target

The distance investigated from this blast condition would create a pressure of 117,211 N/ m^2 onto the upper flange of the beam. This load produces a maximum deflection of 0.66 mm along with a maximum moment of magnitude 48,522 N-m. Figures 15 and 16 represent the deflection and moment profiles, respectively.

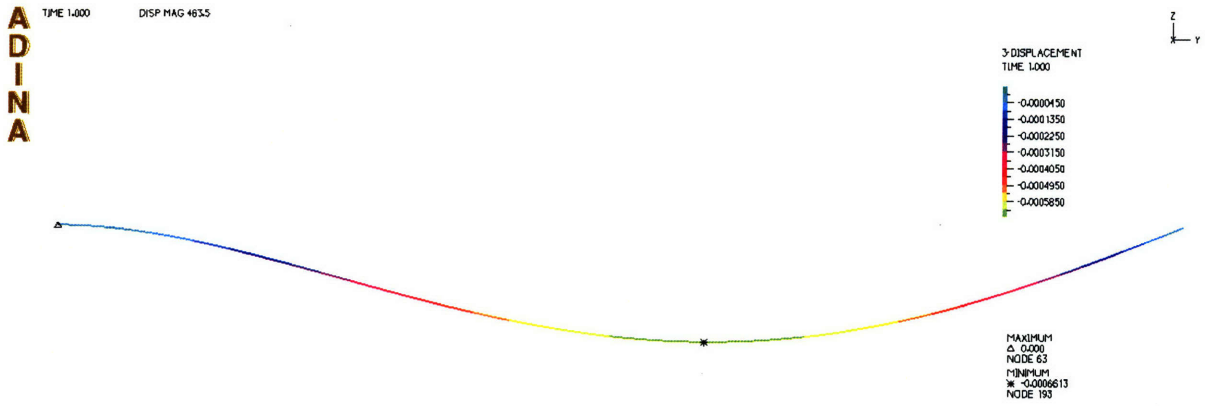

Figure 15– Deflection Profile (61.0 m)

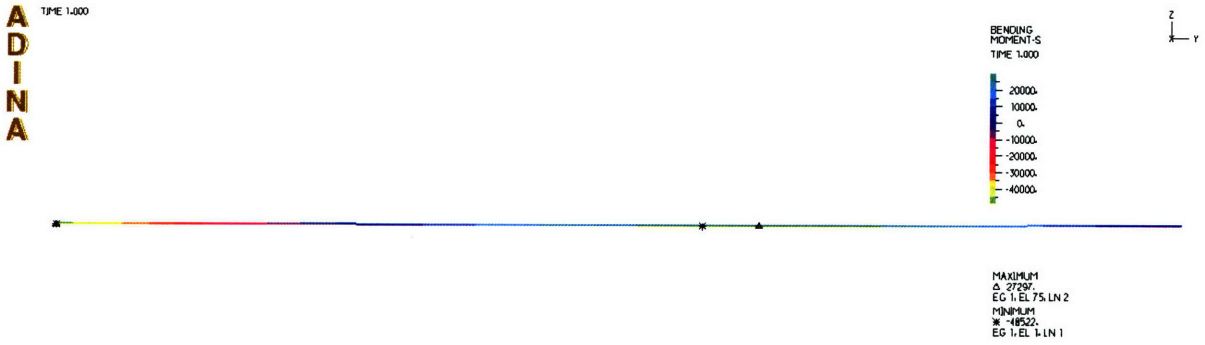

Figure 16– Moment Profile (61 m)

5.3.2.4 Case D: Explosion applied 91.4 m from target

The distance investigated from this blast condition would create a pressure of 20,684 N/ m^2 onto the upper flange of the beam. This load produces a maximum deflection of 0.12 mm along with a maximum moment of magnitude 8,563 N-m. Figures 17 and 18 represent the deflection and moment profiles, respectively.

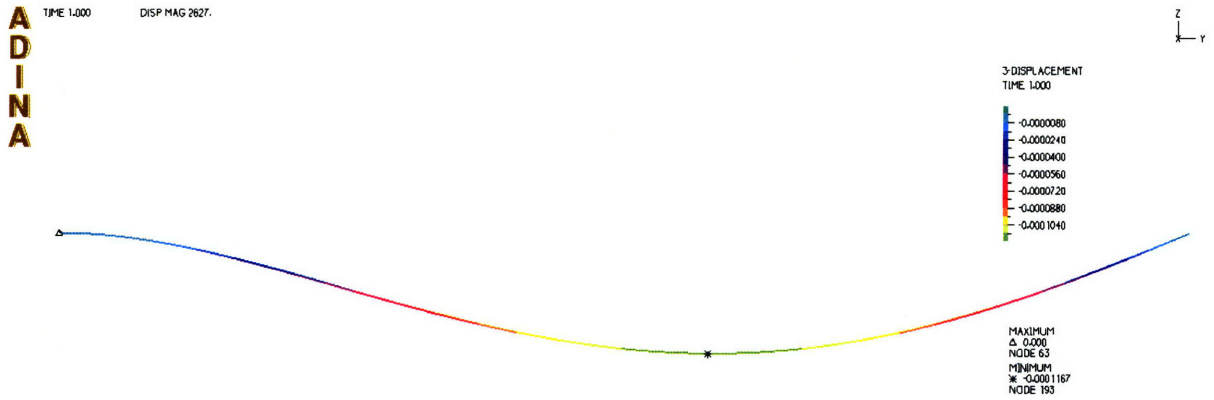

Figure 17- Deflection Profile (91.4 m)

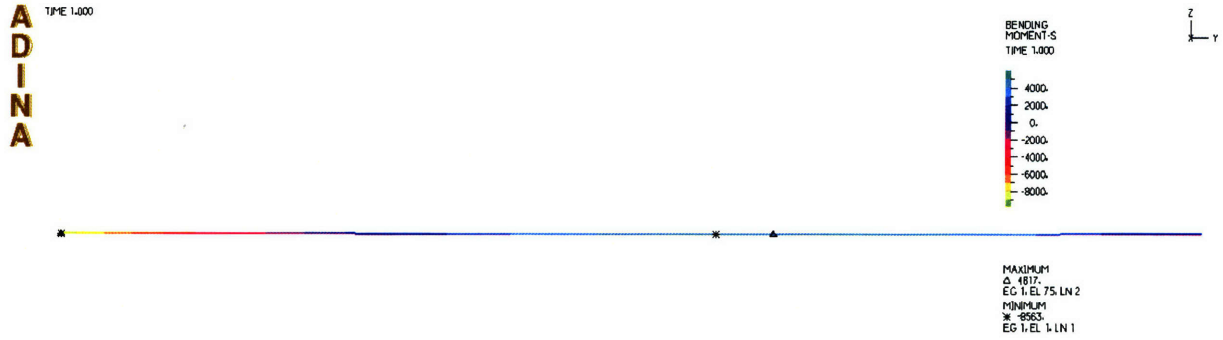

Figure 18- Moment Profile (91.4 m)

After investigating the four cases used in the study, it can be concluded that the standoff distance from a blast is integral in a structure's response. As can be seen from Figure 19, the pressure experienced by the member from the initial explosion greatly decreases as distance increases.

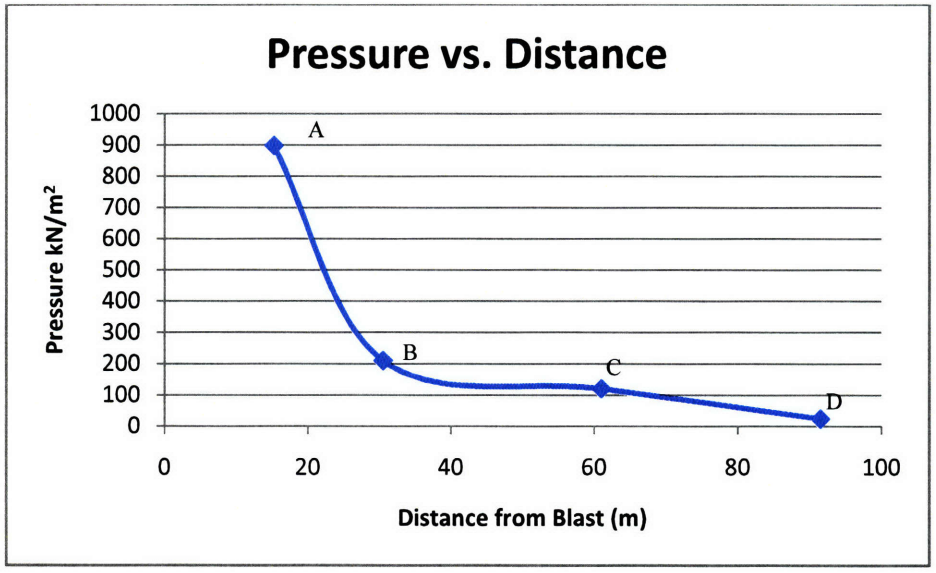

Figure 19- Blast Pressure vs. Distance from Blast

The steep slope inherent from Case A to Case B demonstrates the rapid pressure deterioration experienced by the structure over a short span. Increasing the distance by a factor of two (15.2 m to 30.4 m) dissipated the pressure 77%. Since the respective moments and deflections are linearly related to the blast pressure, they will also experience a tremendous decrease. Thus, the independent components, along with the entire structure will experience less of an impact from an explosive load when a greater standoff distance is provided.

6 Cost Efficient Solutions

When utilizing high-strength materials and composites, it is important to understand that there is an increase in cost for each material. For this reason, engineers cannot design bridges entirely with these new age materials. The structures would then be impervious to large blasts and the fires that ensue, but the entire project would be economically unfeasible. As a result, one should only design critical members with these pricier, stronger materials. After developing the design for a bridge, one should investigate the components that contain the largest forces and ones that may cause a bridge to fail due to lack of redundancy. When these key locations are defined, one should then utilize the high-strength concretes and fiber reinforcements in their designs. Therefore the ensuing blast would not cause these members to experience the high deformations

or forces necessary to initiate failure of the bridge. Also, if the bridge is already in use, these critical members should be covered with a layer of fire-proof coating to prevent the structure from experiencing any major failures should a fire develop.

Areas which are vulnerable to dynamic loads and integral in supporting the structure should be fitted for foam cladding. Main towers and columns should be the only elements that are considered for this composite material due to their importance in the bridge's structural integrity. The energy dissipated by the foam cladding would reduce the response of the bridge to a minimum, and allow the structure to maintain its strength after the blast has been applied.

A great deal of destruction occurs to bridges when blasts take place beneath the deck due to the increase in pressure in confined areas. A simple solution to alleviate this problem would have to take place in the preliminary design stages for a bridge. The scope of work should entail a bridge design that eliminates all dangerous confined areas, which would therefore reduce the amount of damage should an explosion take place. If an engineer notices girders being placed too closely together in areas of high boater traffic, he should design for larger girders that are spaced further apart, thus reducing the amount of blast-enhancing areas. Also, instead of connecting a bridge to land on an incline, a simple excavation and the construction of a retaining wall will eliminate a typical confined area. Figure 20 demonstrates the removal of a potentially dangerous confinement area through the incorporation of a retaining wall.

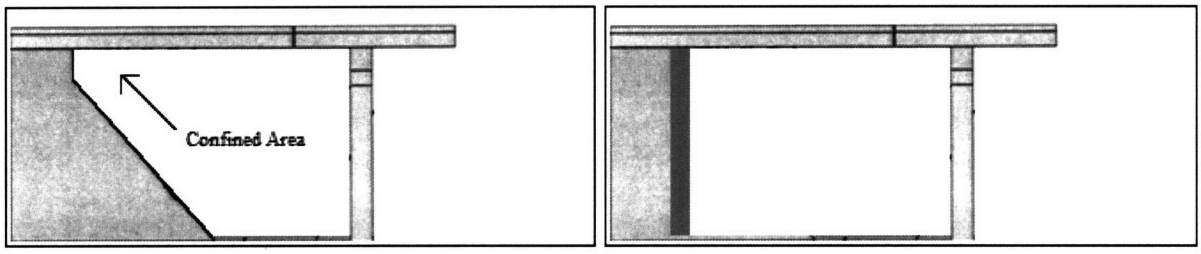

Figure 20- Confined Area Compared to Vertical Retaining Wall (adapted from [1])

Another possible solution could be constructing bridges with a higher vertical clearance. If the engineer knows that the specific waterway will carry immense boater traffic, thus increasing the probability of an accident and explosion, he should alter the design to have a slightly higher vertical clearance for this area. This technique forces the blast to cover a greater volume (less confinement), while experiencing a natural damping from the increased standoff distance.

7 Conclusion

Although it is impossible to predict the magnitude of a blast from a terrorist, a probability model can be developed to approximate the expected blast load a particular structure may encounter. When the magnitude is defined, one can observe how the structure reacts when this load is applied at the critical supports. Using new composite and high-strength materials allows the bridge not only to endure a larger load, but also dissipates the energy so other components do not encounter such high forces. Another positive aspect of these materials is their resistance against cracking and producing dangerous pieces of debris when a blast occurs.

In order to keep the project costs low, engineers should investigate the usage of these materials in crucial areas of the bridge. When these areas are subject to the impulse created from a blast, the overall dynamic response of the bridge will be minimized due to the high performance of the materials.

Other blast resisting techniques that engineers could take advantage of are reducing blast enhancing areas and increasing the vertical distance from a potentially dangerous blast zone. Allowing areas of the bridge to be more widespread will enable the blast to naturally dissipate, and have less effect on the components when applied.

8 References

Chen, Pu-Woei, and D. L. Chung. "Carbon Fiber Reinforced Concrete for Smart Structures Capable Non-Destructive Flaw Detection." (1993): 22-30. 1 May 2008.

Han, Lin-Hai, Jing-Si Huo, and Yong-Chang Wang. "Behavior of Steel Beam to Concrete-Filled Steel Tubular Column Connections After Exposure to Fire." Journal of Structural Engineering (2007): 800-814. ASCE. MIT. MIT Library, Cambridge. 18 Nov. 2007.

Lee, Seung-Hoon. "Ultra HighStrength Concrete Composition." Ultra High Strength Concrete Composition. 31 May 2007. World Intellectual Property Organization. 5 Apr. 2008 <http://www.wipo.int/pctdb/en/wo.jsp?wo=2007061266&IA=WO2007061266&DISPLAY=DESC>.

Mays, G C., and P D. Smith. Blast Effects on Buildings. London: Thomas Telford Publications, 1995. 1-121.

McCallen, David, Bill Wattenburg, Patrick Lewis, and Pete Mote. "Evaluation of an Expedient Terrorist Vehicle Barrier." ASCE: 1-12. 1 Apr. 2008.

Ngo, Tuan, Priyan Mendis, and Ted Krauthammer. "Behavior of Ultrahigh-Strength Prestressed Concrete Panels Subjected to Blast Loading." Journal of Structural Engineering (2007): 1582-1590. ASCE. MIT. MIT Library, Cambridge. 20 Nov. 2007.

Sakumoto, Y., T. Okada, M. Yoshida, and S. Tasaka. "Fire Resistance of Concrete-Filled, Fire-Resistant Steel-Tube Columns." Journal of Materials in Civil Engineering (1994): 89-104. ASCE. MIT. MIT Library, Cambridge. 1 May 2008.

Topcu, Ilker B., and Cenk Karakurt. "Properties of Reinforced Concrete Steel Rebars Exposed to High Temperatures." ASCE (2008): 1-4. ASCE. MIT Library, Cambridge. 12 Apr. 2008.

Uddin, Nasim, Kedar V. Shelar, and Fouad Fouad. "Impact Response of Autoclave Aerated Concrete/FRP Sandwich Structures." Structures 2006 (2006): 1-10. ASCE. MIT Library, Cambridge. 18 Apr. 2008.

William, Kaspar, Lee Keun, Jaesung Lee, and Yunping Xi. "Issues of Thermal Collapse Analysis of Reinforced Concrete Structures." (2006): 1-12. ASCE. Cambridge.

Williamson, Eric B., and David G. Wingett. "Risk Management and Design of Critical Bridges for Terrorist Attacks." Journal of Bridge Engineering (2005): 96-106. ASCE. MIT. Barker Library, Cambridge. Dec. 2007.

Winget, David, Kirk A. Marchand, and Eric B. Williamson. "Analysis and Design of Critical Bridges Subjected to Blast Loads." Journal of Structural Engineering (2005): 1243-1245. ASCE. MIT. MIT Library, Cambridge. 22 Mar. 2008.

Ye, Z. Q., and G. W. Ma. "Effects of Foam Claddings for Structure Protection Against Blast Loads." Journal of Engineering Mechanics (2007): 41-47. ASCE. MIT

9 Figure and Table References

[1] Winget, David, Kirk A. Marchand, and Eric B. Williamson. "Analysis and Design of Critical Bridges Subjected to Blast Loads." Journal of Structural Engineering (2005): 1243-1245. ASCE. MIT. MIT Library, Cambridge. 22 Mar. 2008.

[2] Williamson, Eric B., and David G. Wingett. "Risk Management and Design of Critical Bridges for Terrorist Attacks." Journal of Bridge Engineering (2005): 96-106. ASCE. MIT. Barker Library, Cambridge. Dec. 2007.

[3] Ye, Z. Q., and G. W. Ma. "Effects of Foam Claddings for Structure Protection Against Blast Loads." Journal of Engineering Mechanics (2007): 41-47. ASCE. MIT

[4] Ngo, Tuan, Priyan Mendis, and Ted Krauthammer. "Behavior of Ultrahigh-Strength Prestressed Concrete Panels Subjected to Blast Loading." Journal of Structural Engineering (2007): 1582-1590. ASCE. MIT. MIT Library, Cambridge. 20 Nov. 2007.

[5] Uddin, Nasim, Kedar V. Shelar, and Fouad Fouad. "Impact Response of Autoclave Aerated Concrete/FRP Sandwich Structures." Structures 2006 (2006): 1-10. ASCE. MIT Library, Cambridge. 18 Apr. 2008.

[6] Sakumoto, Y., T. Okada, M. Yoshida, and S. Tasaka. "Fire Resistance of Concrete-Filled, Fire-Resistant Steel-Tube Columns." Journal of Materials in Civil Engineering (1994): 89-104. ASCE. MIT. MIT Library, Cambridge. 1 May 2008.

10 Appendix A- Tendencies of Heated Steel

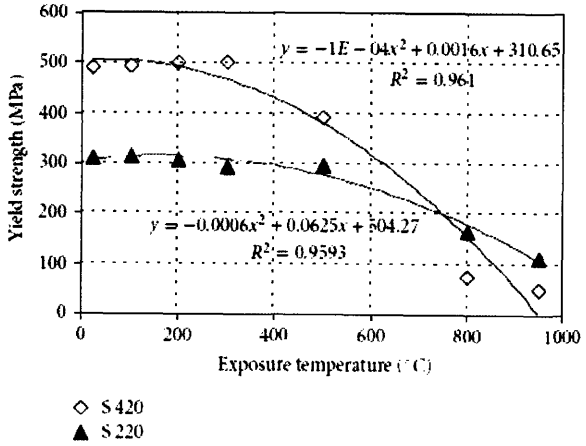

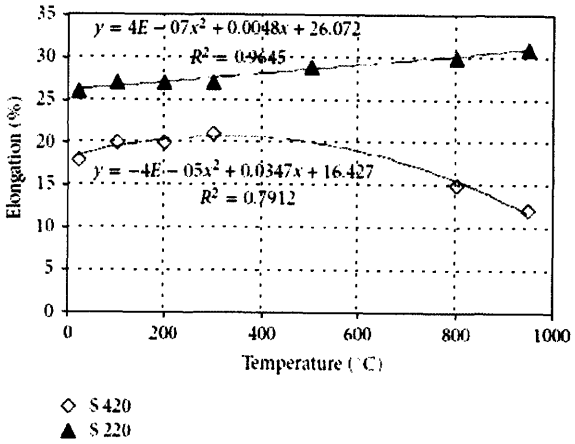

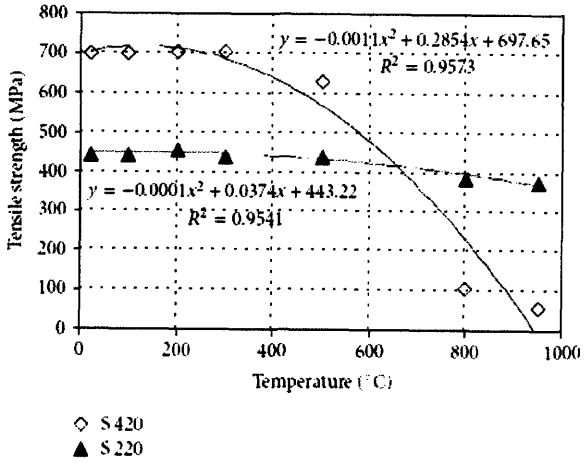

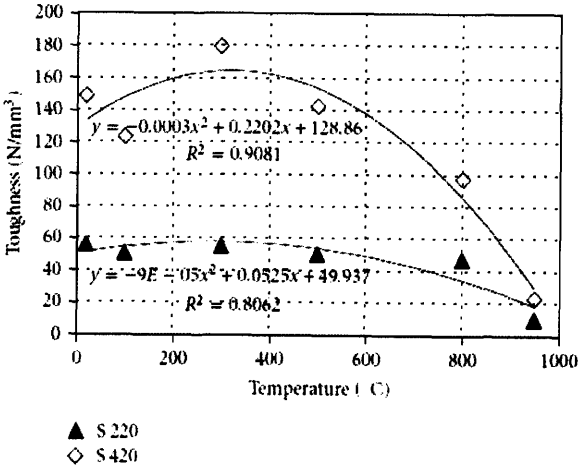

11 Appendix B- Motion Equation Derivation

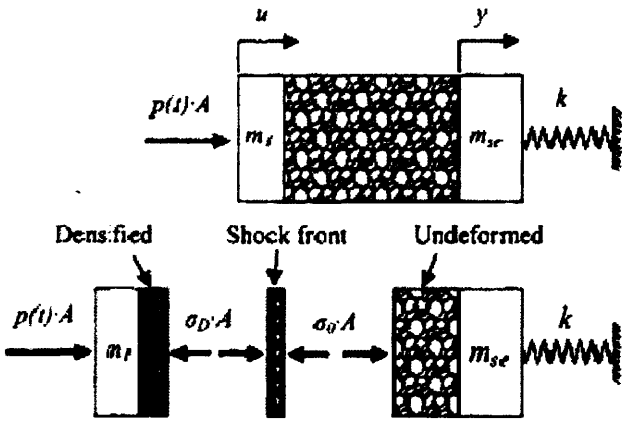

1) Simplified Equation of Motion:

$$m_{se}\ddot{y} + ky = p(t)A$$

2) Conserved mass of densified part of foam layer:

$$\Delta m = \frac{\rho A}{\varepsilon_D}(u - y)$$

3) Stress jump across shock wave front:

$$\sigma_D = \sigma_0 + \frac{\rho}{\varepsilon_D}(\dot{u} - \dot{y})^2$$

4) Plugging into Newton's second law of motion:

$$[m_1 + \Delta m]\ddot{u} + (\sigma_D - p(t))A = 0$$

5) Plugging equations 2 and 3 into equation four yields:

$$\left[m_1 + \frac{\rho A}{\varepsilon_D}(u - y)\right]\ddot{u} + \frac{\rho A}{\varepsilon_D}(\dot{u} - \dot{y})^2 + (\sigma_0 - p(t))A = 0$$

6) Equation of motion for undeformed part of foam layer.

$$\left[m_f - \frac{\rho A}{\varepsilon_D}(u - y) + m_{se}\right]\ddot{y} + ky - \sigma_0 A = 0$$

7) Simultaneously solving equation 5 and 6, the motion equation can be simplified as follows.

$$[m_1 + m_f + m_{se}]\ddot{y} + ky - p(t)A = 0$$

Specimen number (1)	TEST CONDITIONS: Loading Conditions: Axial force ratio (2)	Load (kN) (3)	N_0 (kN) (4)	Load ratio (5)	Eccentricity (mm) (6)	Protection: Type[a] (7)	Thickness (mm) (8)	Time to Reach Temperature (min): 350°C (9)	600°C (10)	TEST RESULTS: Condition (11)	Time (min) (12)	Avg. steel temp. (°C) (13)	Concrete temperature: Close to steel tube (°C) (14)	At center of column (°C) (15)	Axial elongation (mm) (16)	Rate of shortening (mm/min) (17)	Horizontal deflection (mm) (18)
(a) FR Steel																	
R3E0-NI	0.3	2,020	6,730	0.68	None	N	—	7	17	End of elongation	16	593	46	20	17.3	—	—
R3E0-NI	0.3	2,020	6,730	0.68	None	N	—	7	17	Failure	33	766	—	42	−18.7	6.0	—
R2E0-CT	0.2	1,350	6,730	0.45	None	C	5.6	28	107	End of elongation	119	619	272	118	21.3	—	—
R2E0-CT	0.2	1,350	6,730	0.45	None	C	5.6	28	107	Failure	180	726	369	129	2.1	0.2	—
R3E0-CT	0.3	2,020	6,730	0.68	None	C	5.7	29	110	End of elongation	96	560	256	133	16.7	—	—
R3E0-CT	0.3	2,020	6,730	0.68	None	C	5.7	29	110	Failure	166	—	424	136	−3.9	0.3	—
R2E1-CT	0.2	1,350	6,730	0.45	30	C	5.8	30	103	End of elongation	121	639	260	—	21.9	—	6.2
R2E1-CT	0.2	1,350	6,730	0.45	30	C	5.8	30	103	Failure	148	702	314	119	14.8	4.4	91.7
R3E1-CT	0.3	2,020	6,730	0.68	30	C	5.4	23	93	End of elongation	82	568	169	111	14.4	—	9.0
R3E1-CT	0.3	2,020	6,730	0.68	30	C	5.4	23	93	Failure	98	612	215	111	13.2	0.4	20.9
R3E0-FP	0.3	2,020	6,730	0.68	None	P	1.0	34	130	End of elongation	123	582	—	—	18.2	—	—
R3E0-FP	0.3	2,020	6,730	0.68	None	P	1.0	34	130	Failure	188	733	—	—	−15.6	2.5	—
R3E1-FP	0.3	2,020	6,730	0.68	30	P	1.0	20	114	End of elongation	119	614	252	110	16.4	—	3.9
R3E1-FP	0.3	2,020	6,730	0.68	30	P	1.0	20	114	Failure	134	650	290	111	11.4	3.5	25.5
(b) Conventional Steel																	
R3E0-CTX	0.295	2,020	6,840	0.66	None	C	5.7	30	110	End of elongation	64	488	164	102	10.8	—	—
R3E0-CTX	0.295	2,020	6,840	0.66	None	C	5.7	30	110	Failure	194	761	441	134	−17.8	7.3	—
R3E1-CTX	0.328	2,240	6,840	0.73	30	C	5.7	26	—	End of elongation	47	447	168	30	6.0	—	18.1
R3E1-CTX	0.328	2,240	6,840	0.73	30	C	5.7	26	—	Failure	88	565	290	108	1.1	1.0	55.3

[a]N = unprotected, C = ceramic protection, P = intumescent coating.